THE RHIC LATTICE*

S.Y. Lee, J. Claus, E.D. Courant, G.F. Dell, H. Hahn,
G. Parzen and A.G. Ruggiero
Brookhaven National Laboratory
Upton, New York 11973

Abstract

An antisymmetric lattice for the proposed Relativistic Heavy Ion Collider at Brookhaven National Laboratory is presented. It has been designed to have (1) an energy range from 7 GeV/amu up to 100 GeV/amu; (2) a good tunability of β* and betatron tune; (3) capability of operating unequal species, for example, proton on gold. Suppression of structure resonances is achieved by proper choice of the phase advances across the insertions and the arc cells.

Introduction

Recent progress in theoretical and experimental discoveries in nuclear and particle physics points to the importance of physics made available by heavy ion collisions.[1-2] A dedicated Relativistic Heavy Ion Collider (RHIC) has been proposed at this Laboratory.[3] The design for RHIC satisfies a number of requirements: (1) covers the energy interval from 7 GeV/amu up to 100 GeV/amu, (2) a luminosity of 10^{25}-10^{27}/cm^{2}sec for heavy ions such as gold on gold and luminosity of 10^{31}-10^{32}/cm^{2}sec for proton on proton, (3) a ± 10 m free space in the crossing region for experimental equipment, (4) allows operation with unequal species such as proton on gold, (5) capacity for changing β* independently at each crossing point. Most importantly, the accelerator fits into the existing CBA tunnel.

Heavy ions are characterized by small values of Q/A and large values of Q^2/A, where Q and A are charge and mass numbers of ions. Large intrabeam Coulomb scattering, due to large (Q^2/A), requires strong focusing for the beam particles in order to minimize magnet aperture requirements. Therefore the transition energy of the machine is correspondingly high (γ_t = 25). The RHIC injection energy is determined by the maximum B_ρ value available from the AGS, where $B_\rho \cong 100$ Tm or $\gamma_{inj} \cong 12$ for a Gold beam. It is proved impractical to find a lattice which would avoid acceleration through the transition energy. On the other hand, since Landau damping becomes ineffective at the transition energy, it appears preferable to have a low transition energy γ_t to control the total growth of the longitudinal phase space area.[6] Careful studies including all the other aspects such as rate of acceleration, r.f. parameters, and aperture of magnets have been performed to choose an appropriate γ_t and tune. From these studies, it appears that the longitudinal momentum spread of the bunched beam at transition is about Δp/p ≅ 1%. Thus an accelerator with good chromatic properties is important.[7]

In this paper, we present an improved version of RHIC lattice which satisfies these constraints. We discuss the ring structure, the regular cells in the arc, the insertion layout and the betatron amplitude functions, and the stopband bandwidths of the structure resonances and a method of minimizing the effects of these stopbands.

RHIC Ring Structure

Each of the two rings of RHIC is composed of six arcs and six insertions interconnecting these arcs with horizontal crossing. Each arc consists of 12 FODO cells, and each half insertion has a dispersion suppression section, a quadrupole doublet and triplet for β* matching and two dipoles to separate the counter-rotating beams. The polarity sequence of all quadrupoles is antisymmetric with respect to all crossing points. However the sequence is symmetric with respect to the arc centers.

We have chosen π/2 phase advance for each FODO cell of length 29.6 m. This focusing strength is adequate for maintaining the beam size within the available aperture in the presence of the intrabeam Coulomb scattering. At 90° phase advance in each cell with 12 cells per arc, the contribution of systematic chromatic structure resonance stopbands due to quadrupoles and sextupoles is also minimized. The radial separation between the beam centerline in the two rings of the arc is 90 cm for the convenience of magnet construction. Table I lists relevant parameters for these FODO cells.

Table I. Principal Characteristics of Arc Cells

	Inner Arc		Outer Arc
Length (m)	29.5871		29.6571
Deflection Angle (mrad)		77.7007	
Average radius of curvature (m)	380.7928		381.6838
Distance between centerlines (m)		0.9	
Dipole strength (rad)		0.038850	
Quadrupole strength (m^{-1})		0.0995/-0.0093	
Betatron phase adv.		0.25±.005	
$\hat{\beta}_{H,V}/\check{\beta}_{H,V}$ in quad. midplanes (m)		50.0/8.5	
$\hat{X}_p/\check{X}_p$ in quad. midplanes (m)		1.53/.74	

Insertions

The geometry of the insertion is composed of (1) a dispersion matching section (Q9, Q8, Q7, BS2, Q6, BS1 and Q5), (2) a straight betatron function matching section of quadrupole doublet Q5, and Q4 and a triplet lens Q3, Q2 and Q1; and (3) the beam crossing dipoles BC2 and BC1. Figure 1 shows the detailed geometry of the insertion on one side of the crossing point (CR). The other half of the insertion is mirror symmetric in the geometric magnet distribution. BS1 of the inner and outer insertions serve also to bring the separation between the beams to 35 cm at the edge of BC2. The magnets Q3, Q2, Q1 and BC2 of inner and outer insertions sit in the common vacuum vessels. All quadrupole magnets in the insertions are separately adjustable, BS1 and BS2 are in series with the arc dipoles and BC1 is common to both beams. Figure 2 shows the detailed BC1 and BC2 configuration. The collision of unequal species is achieved by exciting BC2 in each of two rings differently with a common field of BC1.[8] Figure 3 shows the betatron and dispersion functions in the insertion region, respectively.

β* can be adjusted in the range 3 m ≤ β* < 10 m by changing the gradients of the insertion quadrupoles without changing the transfer matrix across the insertion. This has been demonstrated in a smooth continuous fashion. Figure 4 shows the maximum β function, $\hat{\beta}$, and the natural chromaticity, χ_N, in the insertion as a function of β*. The six arcs contribute −24 units of natural chromaticity. The contributions from six insertions varies from −16 to −33 for β* from 10 m to 3 m. In the case of protons, the emittance growth due to intrabeam scattering is small and the actual emittance is also small at top energy with the consequence that larger $\hat{\beta}$ up to 2400 m are acceptable. Thus β* can be reduced to about 0.5 m.

Structure Resonances

The stopband width of the half-integer structure resonances for off-momentum particles is given by

$$\Delta\nu_{2n} = \frac{1}{2\pi}\left|\int \beta(\kappa-\delta' X_p)e^{-i2n\psi}ds\right| = \frac{|J_{2n}|}{2\pi}\frac{\Delta p}{p} \qquad (1)$$

*Work performed under the auspices of the U.S. Department of Energy

where $\kappa = B'/B_\rho$, $\kappa' = B''/B_\rho$, β and X_p are the beta and dispersion functions, and $\psi = \int ds/v\beta$ is the betatron phase. The integral J_{2n} can be decomposed into contributions from inner and outer arcs, A_I and A_O, and from inner to outer and outer to inner insertions, C_{IO} and C_{OI}, respectively, i.e.,

$$J_{2n} = 3\left(J_{2n}(A_I) - J_{2n}(A_O) + J_{2n}(C_{IO}) - J_{2n}(C_{OI})\right) \tag{2}$$

at 2n = 51, 57, 63, etc. The factor 3 stems from the superperiodicity of the machine.

For a machine with six-fold superperiodicity, one has $J_{2n}(A_I) = J_{2n}(A_O)$ and $J_{2n}(C_{IO}) = J_{2n}(C_{OI})$. The corresponding half integer stopband width would be zero at ν = 25.5, 28.5 and 31.5 respectively.

For a machine with three-fold superperiodicity, we have to choose the phase advance in each arc cell such that

$$J_{2n}(A_I) \cong J_{2n}(A_O) \cong 0 \quad \text{and} \quad J_{2n}(C_{IO}) - J_{2n}(C_{OI}) \cong 0\ ; \tag{3}$$

are satisfied. The first part of equation (3) is achieved if the phase advance per cell is 60° or 90° for 12 cells per arc. Since the insertions C_{OI} and C_{IO} are mirror symmetric to each other with respect to the center of the arcs, we have

$$J_{2n}(C_{OI}) = e^{-i4\mu_I\pi}\, J^*_{2n}(C_{IO})\ , \tag{4}$$

where μ_I is the phase advance of each insertion. Therefore, the second part of condition (3) becomes

$$J_{2n}(C_{IO}) - J_{2n}(C_{OI}) = J_{2n}(C_{IO})\left(1 - e^{-4\mu_I\pi+2i\phi}\right) \tag{5}$$

where

$$\phi = \frac{1}{2} \arg \frac{J^*_{2n}(C_{IO})}{J_{2n}(C_{IO})} \tag{6}$$

Thus a proper choice of μ_I, i.e.

$$2\mu_I\pi - \phi = m\pi; \quad m = 0,1,2\ldots\ , \tag{7}$$

leads to cancellation of the half integer stopband for neighboring insertions. In the practical application, the intregal $J_{2n}(C_{IO})$ is dominated by a single quadrupole Q20. The contribution to this integral due to the elements Q1I, Q2I, Q3I tend to cancel each other due to the small advance across these elements. Therefore $\phi \cong 4\mu_{Q20}\pi$. Thus Eq. (7) becomes

$$2\mu_I - 4\mu_{Q20} = 4(\mu_I - \mu_{Q20}) - 2\mu_I = \text{integer} \tag{8}$$

This condition (Eq. (8)) is approximately satisfied in the RHIC design.

The third integer structure resonance can also be minimized by the choice of 90° phase advance per cell, where 12 cells per arc give local cancellation for these resonances. Since a variation of the machine betatron tune is obtained by changing the phase advances per cell, we cannot expect complete cancellation of the third integer structure resonance.

Chromatic Corrections

To correct the chromaticity of the machine, we use 6 families of sextupoles located next to the quadrupoles in the arcs. The focusing sextupoles are organized as alternating $S_F - \Delta_F$ and $S_F + \Delta_F$ in the inner arcs and S_F only sectupoles in the outer arcs. Similarly, the defocusing sextupoles have a single strength S_D in the inner arc and alternating strengths $S_D - \Delta_D$ and $S_D + \Delta_D$ in the outer arcs. By adjusting Δ_F and Δ_D, the variation of betatron amplitudes and tune with $\Delta p/p$ can be minimized. Figure 5 shows the variation of the tune and the beta-function vs $\Delta p/p$.

Mini-β Insertion Concepts

β^* in the RHIC insertion is limited by the emittance growth of the heavy ion beam with large intrabeam coulomb scattering. To increase the luminosity, two pairs of common quadrupoles on both sides of the interaction point can be used to obtain β^* = 1 m with $\hat{\beta}$ = 500 m (or β^* = 0.5 m and $\hat{\beta}$ = 1050 m). Each mini-β insertion contributes −17 units to the naturally chromaticity for β^* = 1 m, i.e. the lattice with one mini-β β^* = 1 m and five β^* = 6 insertions would have chromaticity of −60. Chromatic correction for this situation is important.

γ_T Jump

Because Q/A ≤, 1/2 for all heavy ion species, the energy for heavy ions from the AGS falls below the transition energy of RHIC lattices ($\gamma_T \cong 25$). To cross the transition energy, we may need γ_T jump to the lattice. To obtain a proper γ_T change, two families of quadrupoles at 180° phase advance near the QF's of the regular cell are powered. Figure 5 shows the $\Delta\gamma_T$ as a function of tuning quad strength. The corresponding tune change of the machine is shown on the upper part of the graph.

References

[1] G. Baym, "Major Facilities for Nuclear Physics," Physics Today, **38**, p. 40, March 1985.

[2] "Proc. Third Int. Conf. on Ultra-Relativistic Nucleus-Nucleus Collisions," T. Ludlam, H. Wegner, eds., Nucl. Phys. **A418** (1984).

[3] "RHIC and Quark Matter," BNL 51801 (1986).

[4] A. Piwinsky, Proc. 9th Int. Conf. on High Energy Accelerators, p. 405 (1974); J.D. Bjorken and S.K. Mtingwa, Particle Accelerators, **13**, 115 (1983).

[5] G. Parzen, "Strong Intrabeam Scattering in Proton and Heavy Ion Beams," IEEE Trans. Nucl. Sci. **NS-32**, 2326 (1985).

[6] S.Y. Lee and J.M. Wang, "Microwave Instability Across the Transition Energy," IEEE Trans. Nucl. Sci. **NS-32**, 2323 (1985).

[7] J. Claus, M. Cornacchia, E.D. Courant, G.F. Dell, G. Parzen and A. Garren, IEEE Trans. Nucl. Sci. **NS-30**, 2451 (1983).

[8] S.Y. Lee, J. Claus, E.D. Courant, H. Hahn, G. Parzen, IEEE Trans. Nucl. Sci. **NS-32**, 1626 (1985).

[9] S.Y. Lee, G.F. Dell, H. Hahn and G. Parzen, "The Chromatic Correction in RHIC", Proc. 1987 IEEE Part. Acc. Conf. p. 1328 (1987).

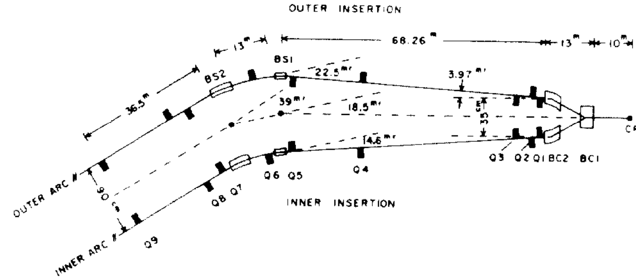

Figure 1. Insertion Layout.

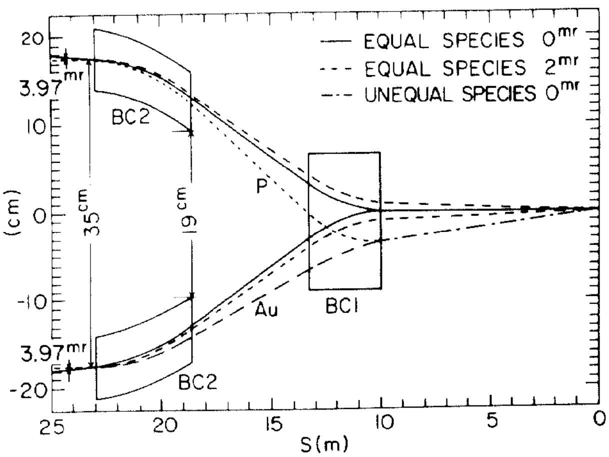

Figure 2. Beams crossing geometry.

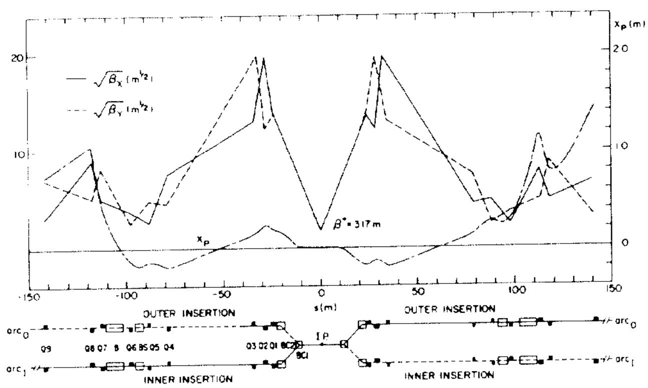

Figure 3. Betatron and dispersion function.

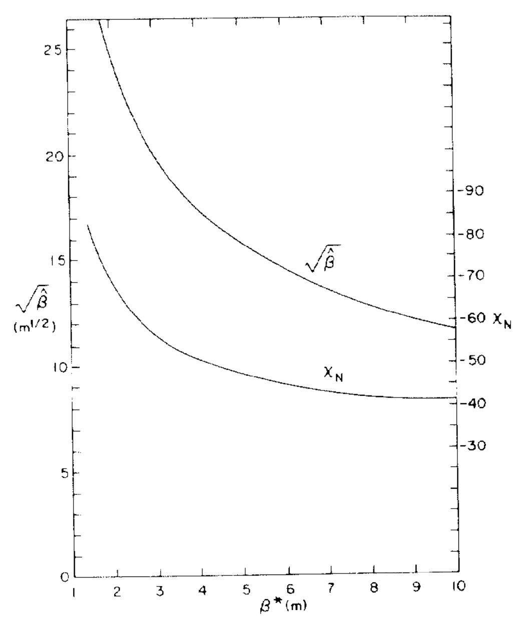

Figure 4. Maximum $\hat{\beta}$ and natural chromaticity χ_N vs β^*.

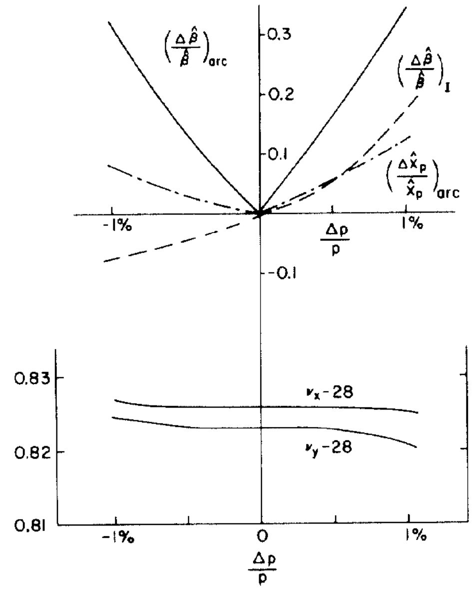

Figure 5. The variation of times and betatron amplitude functions vs momentum for $\beta^* = 6$ m are shown with six family of sextupoles.

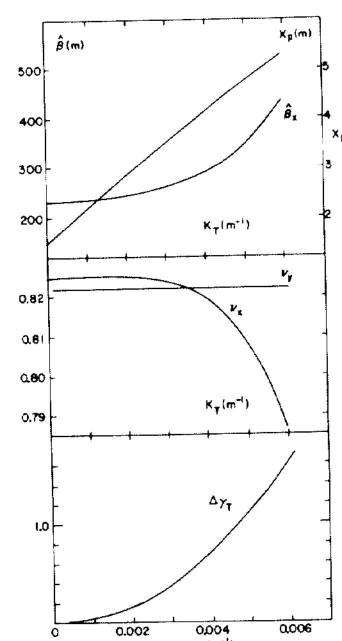

Figure 6. $\Delta\gamma_T$, tunes of the machine, and maximum betatron-function amplitude are shown as a function of the tuning quad strength.